THE ASTROPHYSICAL JOURNAL, 233: 56–66, 1979 October 1

PROPERTIES OF SPIRAL GALAXIES FROM A STOCHASTIC STAR FORMATION MODEL

PHILIP E. SEIDEN AND HUMBERTO GEROLA
IBM Thomas J. Watson Research Center
Received 1979 February 15; accepted 1979 April 10

ABSTRACT

We have examined the properties of model galaxies produced by the stochastic, self-propagating, star-formation model and compared them with those observed in real galaxies. Observations have shown that a good correlation exists between the morphological type of a spiral galaxy and its rotational velocity, color, and gas fraction. We have shown that the stochastic, self-propagating, star-formation model directly correlates the morphological type with the rotation curve, the most important parameter being the maximum rotational velocity. The relative star-formation rates given by the model lead qualitatively to the observed variation of integrated colors and gas fraction as a function of morphological type, as well as to the observed decrease in the density of regions of recent star formation with radius. We show that this model is also capable of giving spiral arms in red plates and discuss the color profiles across spiral arms. Inclusion of the interaction of star formation and the interstellar gas shows that this model is also capable of inducing spiral ordering in the gas.

Subject headings: galaxies: evolution — galaxies: internal motions — galaxies: stellar content — stars: formation

I. INTRODUCTION

The continuing accumulation of data has recently permitted the establishment, on an ever more statistically significant basis, of the existence of correlations among a number of observable properties of galaxies. The understanding of the origin of these correlations and their meaning, however, is still in its early stages. In particular, the following three correlations of the observed properties of galaxies seem well established (de Vaucouleurs 1977). Along the sequence Sa, Sb, Sc, Sd: (1) the maximum rotation velocity of the galaxy decreases; (2) the integrated color becomes bluer; and (3) the fraction of mass in the form of gas increases.

In addition to these correlations, the following important observations have been made in a smaller sample of spirals: (4) the observation of spiral arms in the red plates of galaxies; (5) the observation of spiral arms in the gas of some galaxies, as inferred from 21 cm observations; and (6) the apparent lack of the color gradients across spiral arms.

In Paper I (Gerola and Seiden 1978) we developed the idea that stochastic, self-propagating star formation (SSPSF) is responsible for the creation of aggregates of stars and that the spiral structure displayed by the young stars is caused by the shear of these aggregates induced by differential rotation.

In this paper we point out that this simple model predicts the correct sense of the correlations mentioned above. We take this fact to indicate that many of the properties of spiral galaxies depend on the nature of the major mode of star formation and not on the details of the physics of star formation.

In § II we show that the correlation between maximum velocity of rotation and morphological type is a natural consequence of the model. In § III we point out that the rate of star formation per unit gas density increases monotonically with increasing velocity of rotation, and that properties 2 and 3 mentioned above are a direct consequence of this result. In § IV we discuss the appearance of spiral galaxies as a function of the wavelength band of the observation. Finally, in § V we present a simple model for the interaction of star formation and the interstellar gas, a model indicating that this process can also generate spiral ordering in the gas.

II. MORPHOLOGY

There have been many suggestions that a correlation exists between the morphological type of a galaxy and its rotation curve. In particular, Brosche (1971) has found that the maximum rotational velocity of a galaxy V_M obeys a relation of the type

$$V_m = 290 - 24t, \qquad (1)$$

where t is de Vaucouleurs's parameter for galactic type ($t = 1$ for Sa galaxies, 3 for Sb, 5 for Sc, and 8 for Sc-Irr). Recent observations by Rubin, Ford, and Thonnard (1978) have confirmed this relation for a number of galaxies with flat rotation curves.

In Paper I it was shown that for M81 and M101 the appearance of the model galaxies corresponded well with the appearance of the real galaxies. We have now computed a series of models for flat rotation curves in which all parameters are identical except for the

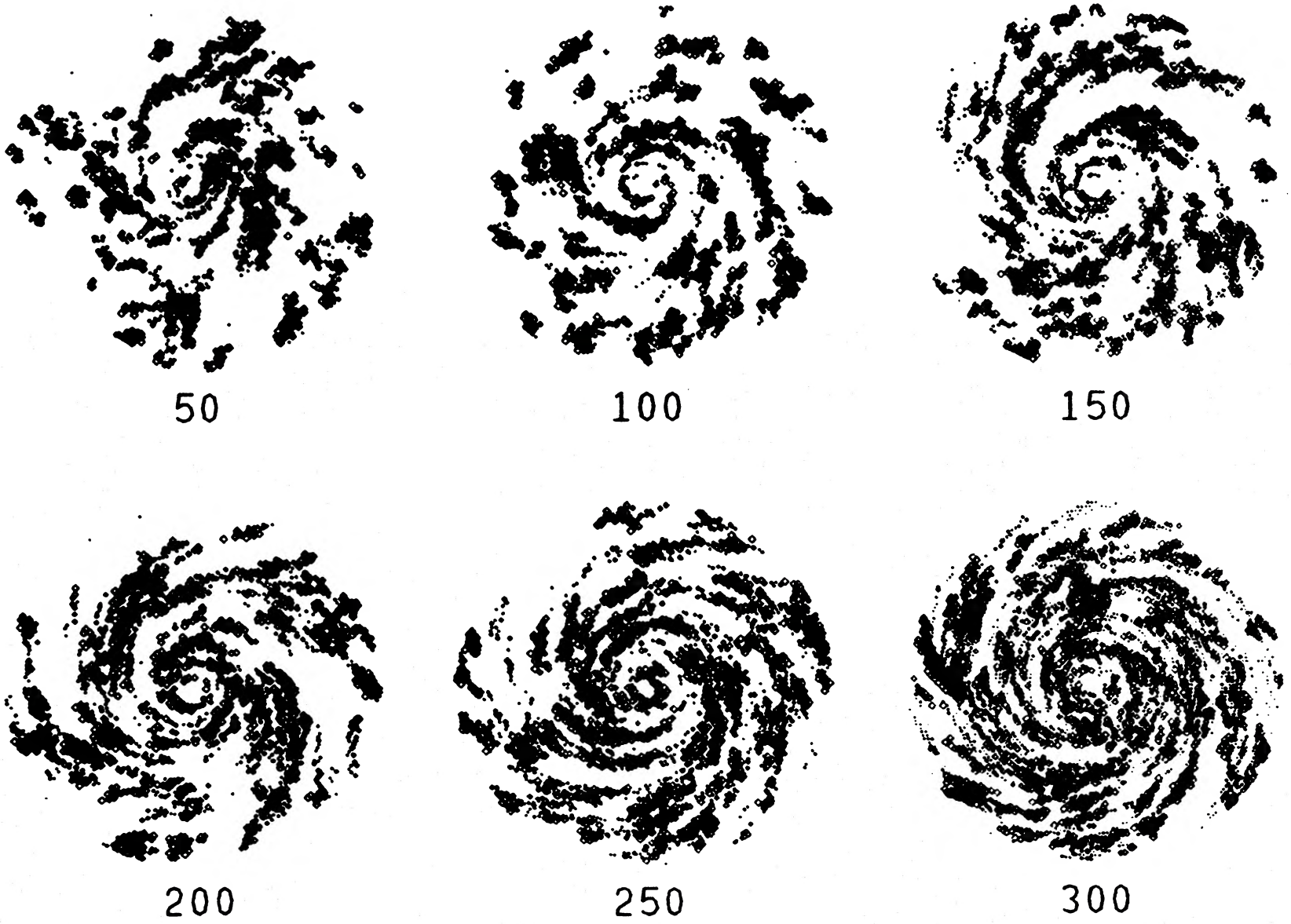

FIG. 1.—Model galaxies having flat rotation curves. The value of the velocity in km s^{-1} is given under each model.

velocity chosen for the rotation curve. We use a set of model parameters similar to those used in Paper I, i.e., we have a two-dimensional polar array of 49 rings (7351 approximately square cells) with a stimulated probability of star formation equal to 0.28, a spontaneous probability equal to 0.0002, and a refractory period of 10 time steps. For a galactic radius of 10 kpc and a supernova remnant or ionization-front velocity of 20 km s^{-1} this choice of parameters gives a time step of 10 million years and a cell size of 200 pc.

Figure 1 shows a typical selection of models generated with flat rotation curves having velocities varying between 50 and 300 km s^{-1}. As can be seen, the models do provide a correlation of the type given by equation (1). The regular progression from the irregular structure of the 50 km s^{-1} model to the very tightly wound Sa type structure at 300 km s^{-1} is apparent in the figure.

In order to provide a quantitative measure of the morphological type, we use an objective procedure for determining the angle of the spiral arms of any particular model. The form usually chosen for fitting the spiral arms of galaxies is a logarithmic spiral, that is,

$$R = R_0 \exp(\phi/\phi_0) . \quad (2)$$

We fit this equation to the models of Figure 1 using ϕ_0 as a fitting parameter. The fitting procedure is based upon the concept of geometric entropy defined in Paper I. To find the geometric entropy, a pattern is first coarse-grained into 3 × 3 blocks and then the entropy is calculated from the population of stars in each block. This quantity is then divided by the entropy of a random array having the same stellar density. The resulting quantity, the geometric entropy, provides a measure of the order of the system (see Paper I or Schulman and Seiden [1978] for the complete mathematical formulation).

The galactic model is rotated backward by the angle ϕ, determined from equation (2), effectively unwinding the spirals. The geometric entropy of the unwound galaxy is then evaluated. The process is carried out for a range of ϕ_0, and the best fit is the value of ϕ_0 that minimizes the geometric entropy, since for it the long spiral sections will have unwound to form shorter but more heavily populated regions. In Figure 2 we show the results of this procedure for the 200 km s^{-1} model of Figure 1. In Figure 3 we show a plot of the value of ϕ_0 for minimum entropy as a function of rotation velocity for all six models of Figure 1. The pitch angle is a strong function of the rotation velocity.

A word of caution is in order on the choice of a logarithmic spiral to represent the form of the spiral arms. We have used this form here because it has usually been considered to be the proper choice for real galaxies. However, it is not at all clear that this is the case. Dzigvashvili and Borchkhadze (1970) examined the spirals in a number of multiple-arm galaxies and have shown that the normal logarithmic spiral is not an appropriate representation. In order to fit the arms the pitch angle of the spiral must vary along the observed arms.

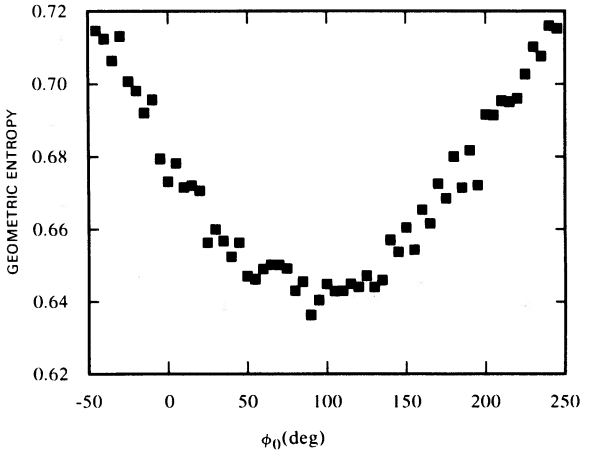

FIG. 2.—Geometric entropy as a function of pitch angle for the unwound 200 km s^{-1} model of Fig. 1. The model is unwound using eq. (2).

For our models it is easy to show that a logarithmic spiral is not the appropriate choice. The angular displacement of a star per time step is given by

$$\phi = \frac{V}{R} t = \frac{V}{R} \frac{C_s}{V_{IF}} , \quad (3)$$

where V is the tangential velocity, t the time step, C_s the cell size, and V_{IF} the average propagation velocity of the shock front that induces star formation in an adjacent region (see Paper I). For a flat rotation curve,

$$\phi R = C_s V / V_{IF} = \text{constant} . \quad (4)$$

Therefore, the appropriate choice for our model is a hyperbolic spiral. The result of Figure 3, that pitch angle is a strong function of rotational velocity, is unaffected by the choice of spiral type. The question of the proper choice for the form of the spirals, both for our models and for real galaxies, as well as a more complete discussion of the use of geometric entropy

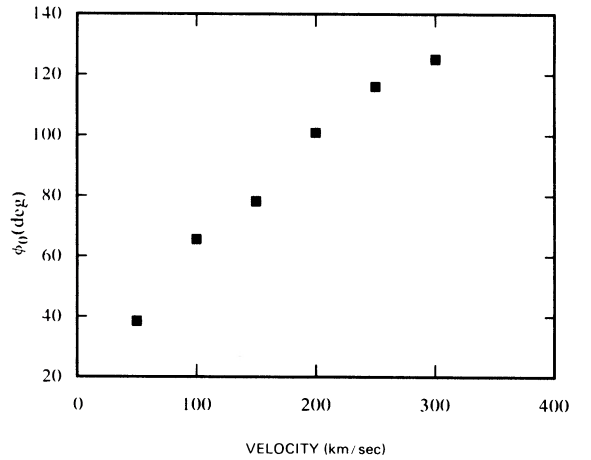

FIG. 3.—Pitch angle for minimum entropy as a function of rotation velocity for the models of Fig. 1.

for the characterization of galaxies, will be the subject of a future paper.

The important result here is that the major parameter determining the morphological type of a normal disk galaxy is the maximum velocity of the rotation curve; it plays the primary role in determining the constant in equation (4). In the simplest case we can regard V_{IF} and C_s as being local parameters primarily involved with the star-formation process itself. That is, C_s is of the order of the association size and V_{IF} is the average velocity at which the signal proceeds from one association to nucleation of the next. If these parameters are independent of galaxy type, equation (4) is a one-parameter equation for morphological type (for flat rotation curves). However, since the spiral form is not logarithmic, the appearance of the galaxy will still depend on its size as well as its rotational velocity. The appeal of a logarithmic spiral is that $d\phi/d \log R =$ constant, so that equal factors of radii will sweep out equal angles. For a hyperbolic spiral this is not true: $d\phi/d \log R \sim R^{-1}$, so that the apparent pitch angle decreases with radius.

Although the SSPSF mechanism is capable of producing many of the observed spiral forms, it should not be assumed that it is the only mechanism active in galaxies. The more-regular two-armed spirals, particularly in barred galaxies, probably involve other mechanisms (Kormendy and Norman 1979). Two-armed spirals occasionally arise from SSPSF, but this statistical appearance would not account for their overwhelming occurrence in barred spirals.

III. RATE OF STAR FORMATION

Once the parameters of the model are given, not only is the morphology established, as shown in the previous section, but the relative rate of star formation per unit gas density is also determined. This last quantity is identifiable with the frequency of newly excited cells per time step. Figure 4 shows the relative star-formation rate of the model as a function of velocity (again for flat rotation curves) and, therefore by the results of § II, as a function of morphological type. These results are obtained while keeping all other model parameters constant. The behavior as a function of all parameters has not yet been completely mapped out; however, the two curves of Figure 4 indicate the range of behavior observed in the region of good spiral structure. Virtually any intermediate curve can be found by a suitable choice of parameters. The behavior is most strongly dependent on the value of the stimulated probability since the star-formation rate is a very strong function of this parameter in the spiral region. A treatment of this behavior in terms of critical phenomena and its implications for the evolution of galaxies has been given by Seiden, Schulman, and Gerola (1979).

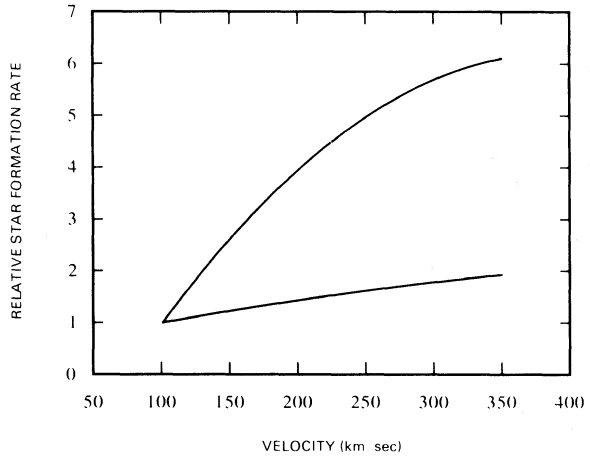

FIG. 4.—Relative star-formation rate as a function of velocity for flat rotation curves (see text for explanation of curves).

The point to be emphasized here is that for all values of the model parameters one finds behavior similar to Figure 4; i.e., as the rotational velocity increases the star-formation rate increases. That this is the case is not hard to understand. The important parameter determined by the rotation curve is the differential rotation, $d\omega/dR$. From equation (4) we can see that for the case of flat rotation curves the differential rotation is directly proportional to the velocity itself. The larger the differential rotation the faster new cells will be brought into contact with active star-forming cells, thereby enlarging the region available for stochastic star propagation. That is, in a differentially rotating disk the neighbors of an active region change continuously, allowing the active region to affect a much larger area than for the case of a rigidly rotating disk.

This dependence of the rate of star formation on the shear is an intrinsic property of the model, independent of the exact details of the physics of the propagation of star formation. It is therefore important to explore its consequences for the correlation between morphological type and other observable properties of galaxies.

a) Radial Distribution of Young Stars

One consequence of this variation of star-formation rate with differential rotation is the radial dependence of the density of young stars. From equation (4) we can see that the differential rotation decreases as $1/R^2$; therefore, we would expect that the star-formation rate would decrease as a function of radius. In Figure 5 we show data for a galaxy having a flat rotation curve with a velocity of 220 km s^{-1} (similar to our Galaxy, as per Knapp, Tremaine, and Gunn 1978). Two points should be noted: one, the fluctuation in the star density can be quite large, and two, as expected, there is a decrease in the average star density as the radius increases.

Observations in our own Galaxy (see Burton 1976 for a review) and in external galaxies (Hodge 1974; Roberts 1975) indicate that tracers of Population I, such as H II regions and supernova remnants, indeed have a radial distribution with negative gradient. Although the values for the observed gradients are

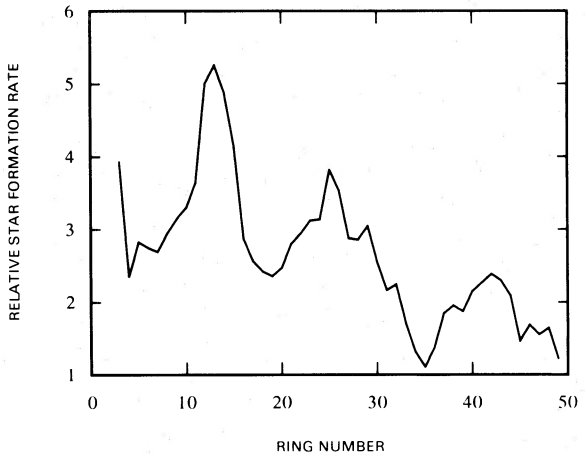

FIG. 5.—Relative star-formation rate as a function of ring number (~radius) for a 49 ring model having a flat rotation curve of 220 km s^{-1}.

quantitatively not very reliable, it appears that the observed distributions are steeper than the one shown in Figure 5. However, the model calculations with a constant P_{st} correspond to a case where the gas fertile for star formation is distributed homogeneously. If the sites of star formation are massive molecular clouds, and if these, at least as in our Galaxy, are concentrated toward the center, one should fold this distribution into the radial distribution of star density that would generate a still steeper gradient in closer agreement with observations.

b) Relative Galactic Colors

Previous theoretical work (see, e.g., Audouze and Tinsley 1976; Searle, Sargent, and Bagnuolo 1973; Larson and Tinsley 1978) suggests that the observed sequence of colors with morphological type mentioned in the introduction can be understood if the sequence Sa-Sb-Sc is also a sequence of decreasing star-formation rate per unit gas density. As discussed above, the stochastic star-formation model predicts just such a sequence. However, previous work has neglected the details of the contribution to integrated colors of the Population II component of the bulge. The sequence Sa-Sc is also, in a statistical sense, a sequence in decreasing bulge to disk ratio; although many exceptions exist, this ratio is in fact used by astronomers to determine the type of galaxies that are seen edge-on. Therefore, the situation with respect to colors remains unclear. It is interesting, in any case, to evaluate how well the star-formation rate given by the SSPSF model can reproduce the observed average sequence of colors with the same simplifying assumptions of the work of Searle, Sargent, and Bagnuolo (1973).

The relative colors can now be calculated from the curves of Figure 4 using the data and methods of Searle, Sargent, and Bagnuolo (1973) or Larson and Tinsley (1978). The results are shown in Table 1 along with the observed average values (de Vaucouleurs 1977). The model only supplies the relative star-formation rates, and the calculation is therefore fitted to the observations for Sd galaxies.

TABLE 1

COLORS AND GAS FRACTION OF SPIRAL GALAXIES

PARAMETERS	GALAXY TYPE Sa	Sb	Sc	Sd
t[a]	1	3	6	8
V (km s^{-1})[b]	266	218	146	98
Observed[a]				
$U - B$	0.27	0.06	−0.19	−0.22
$B - V$	0.70	0.66	0.44	0.42
M_g/M_T	0.01	0.04	0.07	0.12
Local IMF and upper curve of Fig. 4[c]				
$U - B$	−0.06	−0.09	−0.15	−0.20
$B - V$	0.56	0.54	0.48	0.44
M_g/M_T	0.19	0.25	0.45	0.73
Power-law IMF ($\alpha = -2.45$) and upper curve of Fig. 4[c]				
$U - B$	0.35	0.33	0.18	−0.22
$B - V$	0.83	0.82	0.72	0.41
M_g/M_T	2×10^{-5}	10^{-4}	5×10^{-3}	0.12
Power-law IMF ($\alpha = -2.1$) and lower curve of Fig. 4[c]				
$U - B$	−0.03	−0.08	−0.17	−0.22
$B - V$	0.57	0.53	0.46	0.41
M_g/M_T	0.03	0.04	0.08	0.12

[a] de Vaucouleurs 1977.
[b] Equation (1).
[c] See text.

The colors calculated from clusters having a composition determined by the initial mass function in the solar neighborhood (Larson and Tinsley 1978) are considerably bluer than the observed colors both for $U - B$ and $B - V$. One reason for this may be the neglect of the bulge component described above. According to Schweizer (1976) this adds about 0.1 mag to the color for Sb's. This correction brings the theoretical value into much better account with observation.

The calculated color of a galaxy is strongly dependent on the initial mass function (IMF) used for the mass spectrum of the cluster. Searle, Sargent, and Bagnuolo (1973) have tested this dependence by using a power-law IMF and varying the power (α). For $\alpha = -2.45$ they find approximately the same result as found for the local IMF of Larson and Tinsley. In addition, they repeated the calculation for $\alpha = -2.1$. The results for this IMF are also shown in Table 1. The relative star-formation rate represented by the upper curve in Figure 4 gives galaxies much too red, while the lower curve gives galaxies much too blue. It is clear that for this IMF it is possible to find a curve in the allowed region of Figure 4 that will give a good representation of the observed colors.

In sum, although we do not pretend to obtain a quantitative calculation of the relative colors of galaxies, the SSPSF model does provide a star-formation rate that has the proper dependence as a function of morphological type for qualitative agreement. A more extensive analysis of both theory and observation is necessary before a definite conclusion can be made as to how well the colors are accounted for.

c) *Fractional Gas Content*

The same simple calculation described above, with the assumption of no infall of gas into the disk, also determines the fraction of matter remaining in gaseous form in the model galaxy. This fractional gas mass (M_g/M_T) has been observed to be correlated to morphological type (see de Vaucouleurs 1977). A comparison of our results with the observational data of Roberts (1975) (Table 1) shows results similar to those obtained for the colors. For the local IMF the fractional gas mass obtained is much too high. However, for the reduced power-law IMF it is possible to find a relative star-formation rate function that will give the proper fractional gas-mass dependence as well as the proper colors.

IV. SPATIAL DISTRIBUTION OF STELLAR POPULATIONS

According to gravitational theories, spiral structure in galaxies results from the dynamical behavior of the whole galaxy, so that the spiral structure is present in all stars, old and young, and in gas. The present stochastic star-formation model is a local process that directly induces spiral structure in the young stars only, a structure which will be smeared out and disappear as the stars age and disperse (see § V for a discussion of the gas). The identification and separation of star populations of different ages may therefore be a critical test on the nature of the mechanism producing spiral structure.

Observations of spiral galaxies in various color bands (Schweizer 1976) have shown that the appearance of the spiral arms depends on the band used for the observation. In particular, *U* band plates generally show thin and splotchy arms; the most notable features being the bright OB associations and related H II regions. As one proceeds to redder plates the arms become fuller and more continuous. The appearance of prominent arms in the red has been interpreted by some workers as being due to the existence of spiral structure in the old red stars. However, since blue stars also radiate profusely in the red and the supergiant phases of massive stars have their large luminosity peaked in the red, it is not clear that this interpretation is correct.

a) *Multicolor Photometry*

In the stochastic star-formation model the spiral structure is determined by the relatively young stars since the very old red population will be homogenized by the continuous winding up and smearing out of its spiral structure by the galactic differential rotation. The representation of our model, given by pictures like Figure 1, shows only the youngest stars ($\leq 10^8$ years) and completely suppresses the older stars. In order to determine the effect of the older stars we will now plot the luminosity of the model galaxies instead of just the age of the massive stars. To do this we assume that each of our creation events creates a cluster of stars. Struck-Marcel and Tinsley (1978) have calculated the luminosity of such clusters as a function of their age for the photometric bands *U*, *B*, *V*, *R*, *I*, and *K*.[1] We use these results to find the luminosity of each region of our model galaxy from the age of the cluster therein. The results are shown in Figure 6 for the six color bands (the results presented for all of § IV are for the same flat rotation curve with velocity of 220 km s^{-1} discussed in § III*a*). The plots show stars up to 2.55×10^9 years, and the "modeled plates" are "exposed" such that the most luminous clusters in the particular band of interest are saturated, i.e., they have a symbol size filling the area of the cell. The symbol size is then linearly decreased with decreasing intensity.

In the *U* and *B* bands only the youngest and brightest stars show up clearly; clusters older than 4×10^8 are not bright enough to show up at all under the linear intensity scale described above. In the infrared, however, all colors appear. The first line of Table 2 gives the age of the cluster having the smallest symbol visible for the plots of Figure 6. In agreement with observations the spiral structure in the blue bands is rather thin and spotty. For the redder bands the arms fill out, become smoother, and are reduced in contrast with respect to the background. The reduction in contrast occurs because at longer wavelengths the older red clusters begin to appear with appreciable luminosity. However, it is not until we reach the *K*

TABLE 2

AGE AND LIGHT FRACTION OF CLUSTERS NOT SHOWN IN FIGURE 6

Photometric Band	Cluster Age[a] (10^7 years)	Light Fraction[b]
U	41	0.15
B	72	0.27
V	87	0.39
R	99	0.49
I	133	0.55
K	255	0.66

[a] Corresponding to luminosity cutoff of Fig. 6.

[b] Fraction of light due to clusters older than those shown in Fig. 6 (15×10^9 year old galaxy).

[1] Struck-Marcel and Tinsley (1978) reported only the *U*, *B*, *V*, and *K* data. Dr. Struck-Marcel has kindly provided us with the data for the *R* and *I* bands. These were not included in their paper for the following reason. For the *K* band they were able to adjust the results of Tinsley and Gunn (1976) for single-burst models to reproduce the Frogel, Persson, and Aaronson (1977) results for giant elliptical galaxies. This could not be done for *R* and *I* bands since the relevant observations are not available. The expected differences would not affect the conclusions presented here.

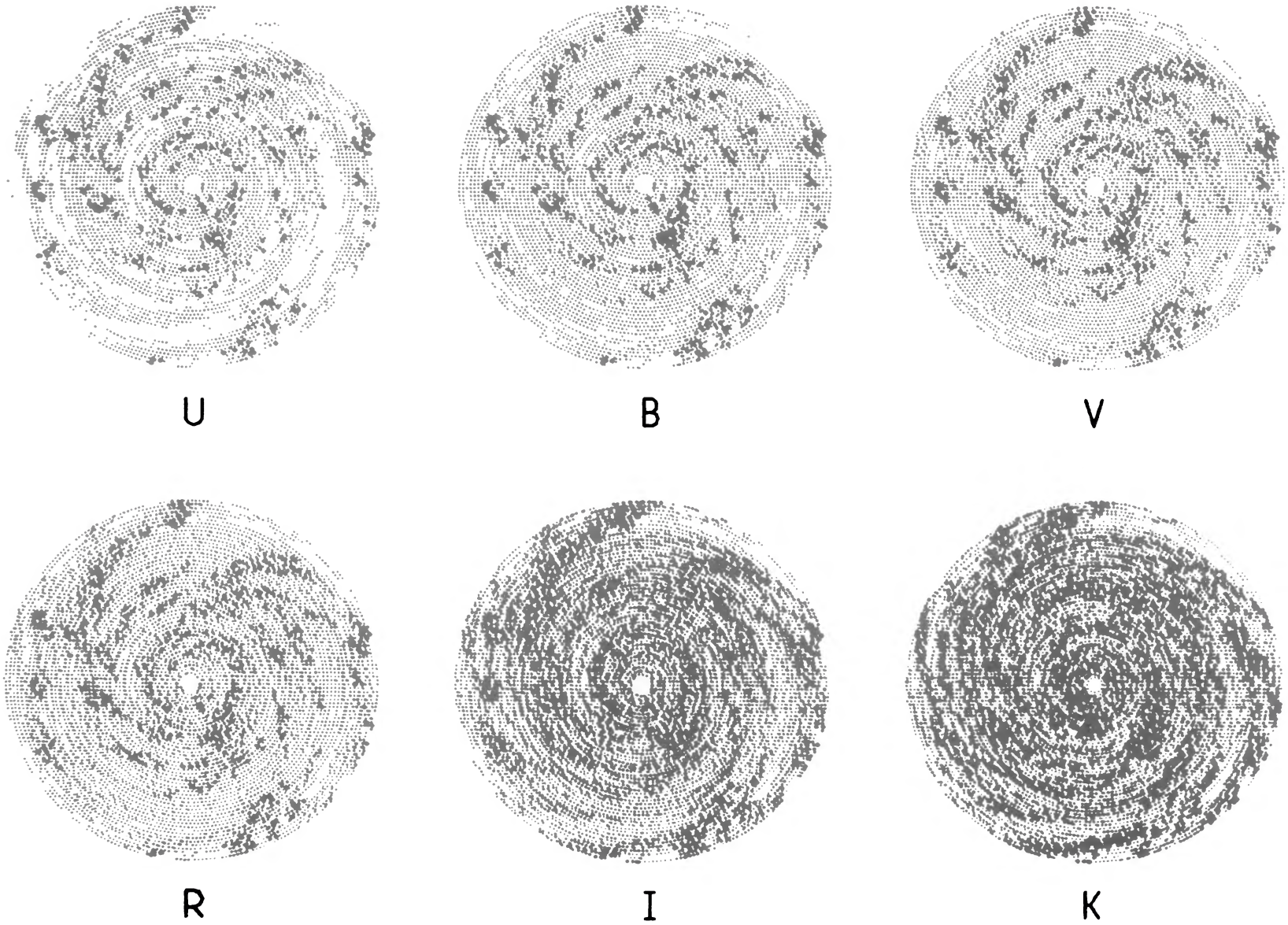

FIG. 6.—Six color photometry for the model of Fig. 5. The letter below each figure denotes the photometric band.

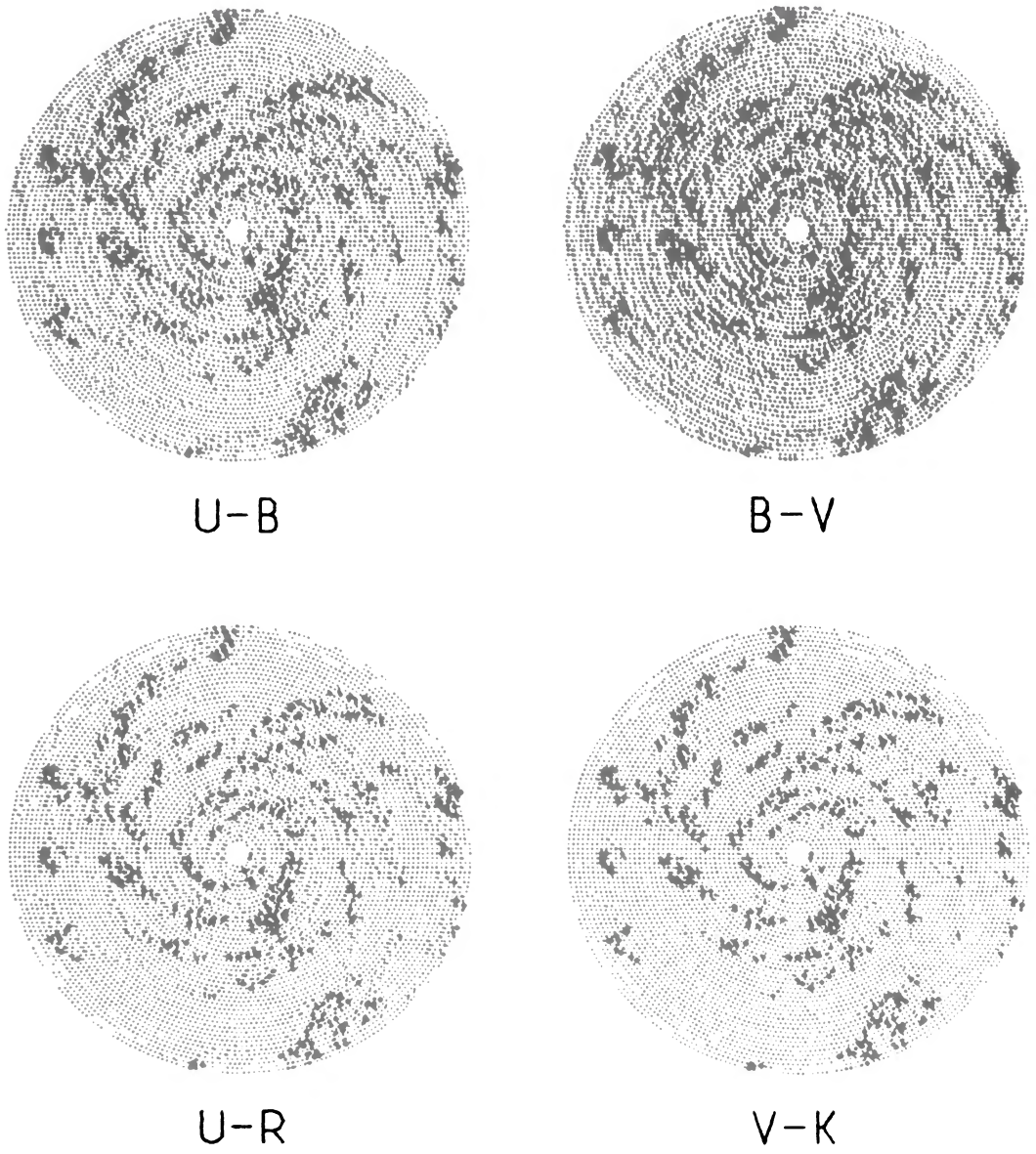

FIG. 7.—Relative color composites for the model of Fig. 5. The letters below each figure denote the photometric bands used.

band that the contrast of the arms has been reduced to such a degree that they become indistinct; and even for this band the spiral structure can be perceived in Figure 6.

The results of Figure 6 show only the youngest cluster for each cell and include only clusters up to 2.55×10^9 years in age. Including all the generated clusters would reduce the contrast of the arms a bit further but would not destroy, at least for R band or shorter wavelengths, the appearance of the spiral structure. Table 2 shows the fraction of light in each band for a 15×10^9 year old galaxy that is due to the clusters not included in Figure 6. Even after including this light the spiral structure in R and perhaps also in I would remain, although the K band arms should be obscured.

The question of the appearance of spiral arms has also been investigated by composite plate synthesis techniques depicting the usual color indices. Figure 7 shows the same model galaxy for four of the more commonly discussed indices. The spiral arms are clearly delineated for all four indices although the contrast is less than for the direct plates themselves.

The conclusion to be drawn from this discussion is that the relative luminosity of the young massive stars in a typical spiral galaxy so dominates the total luminosity that the spirals appear in observations at bands shorter than 2 μm (K band). The appearance of

spiral arms in the red cannot be used as evidence for the existence of arms in the very old disk stars.

b) Color Gradients in Spiral Arms

Recently, good surface color photometric data on spiral galaxies have started to become available. One motivation for these efforts was to test the existence of well-ordered color gradients across spiral arms predicted by a simple interpretation of the spiral density wave theory. In the galaxies observed so far by Schweizer (1976) and by Talbot, Jensen, and Dufour (1978), no systematic color gradient is observed to exist. The situation, as summarized by Schweizer (1976), is that most of the luminosity azimuthal profiles in different color bands are rather symmetric; among the observed asymmetric profiles there is a slight majority of "forward drift" profiles, those predicted by the spiral density wave theory, but in many cases "backward drift" profiles are observed. All three types of profiles appear in each galaxy.

In Figure 8 we show the azimuthal profiles obtained from our model. A simple inspection of this figure indicates that we obtain precisely the same situation as observed. Most of the profiles are symmetric, but asymmetric profiles of both the "forward and backward drift" types are present. Furthermore, it appears that there is a small preponderance of the forward over the backward type. This is probably a consequence of the preferred direction of motion introduced by the differential rotation of the disk. We believe that the approximately symmetrical behavior is an indication of the essentially random direction of propagation of star formation induced by the SSPSF mechanism.

V. A MODEL FOR THE DISTRIBUTION OF GAS

Up to this point the SSPSF model has considered stars only and has always implicitly assumed the existence of uniformly distributed gas from which the stars may be formed. We now want to extend the model to take into account the distribution of the interstellar gas. We will not explicitly consider the dynamics of the gas but we will allow its distribution to be affected by the star-formation process.

In addition to our usual assumption of an initial distribution of stars, we now include an initial distribution of gas (a homogeneous distribution for the results presented here). After a cluster is nucleated in a cell we allow the ionization fronts, stellar winds, and supernova explosions in that cluster to redistribute the cell's gas among its neighbors on the next time step. The gas is also allowed to homogenize by diffusion on a time scale determined by the velocity of sound in the gas (~ 2 km s^{-1}). The probability for star formation is now taken to be proportional to the amount of gas contained in a cell. This procedure lets the gas move about under the influence of the energetic star-evolution processes and confines the creation events to those cells containing sufficient gas for stellar condensation.

Some results of this model calculation are shown in Figure 9. First look at the top two pictures. The stellar arms, seen in the left-hand picture, are well separated. In this case the gas, shown in the right-hand picture, also shows evidence for arms, although the contrast is much reduced. In the bottom of Figure 9, on the other hand, the density of stellar arms is much greater but still clearly resolved, while the arm structure in the gas is obscured. The result is that if the stellar arms are well enough separated the SSPSF model can also show arms in the gas. Since the contrast of these arms is much lower than for the stars the arms are easily washed out by the interference between the gas distributions of closely spaced arms.

Therefore, since we can also obtain spiral arms in the gas by the SSPSF model, the observation of these

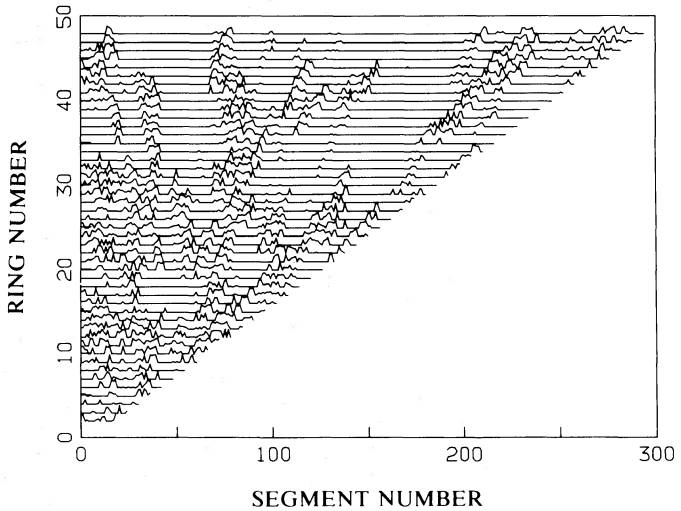

FIG. 8.—Azimuthal variation of cluster age for the model of Fig. 5. The ordinate gives the ring number being plotted ($\sim$radius), while the abscissa gives the segment number along the ring numbered in the rotation direction. The number of segments per ring is $6n$, where n is the ring number. The height of each curve above its zero level is proportional to the inverse age of each cluster.

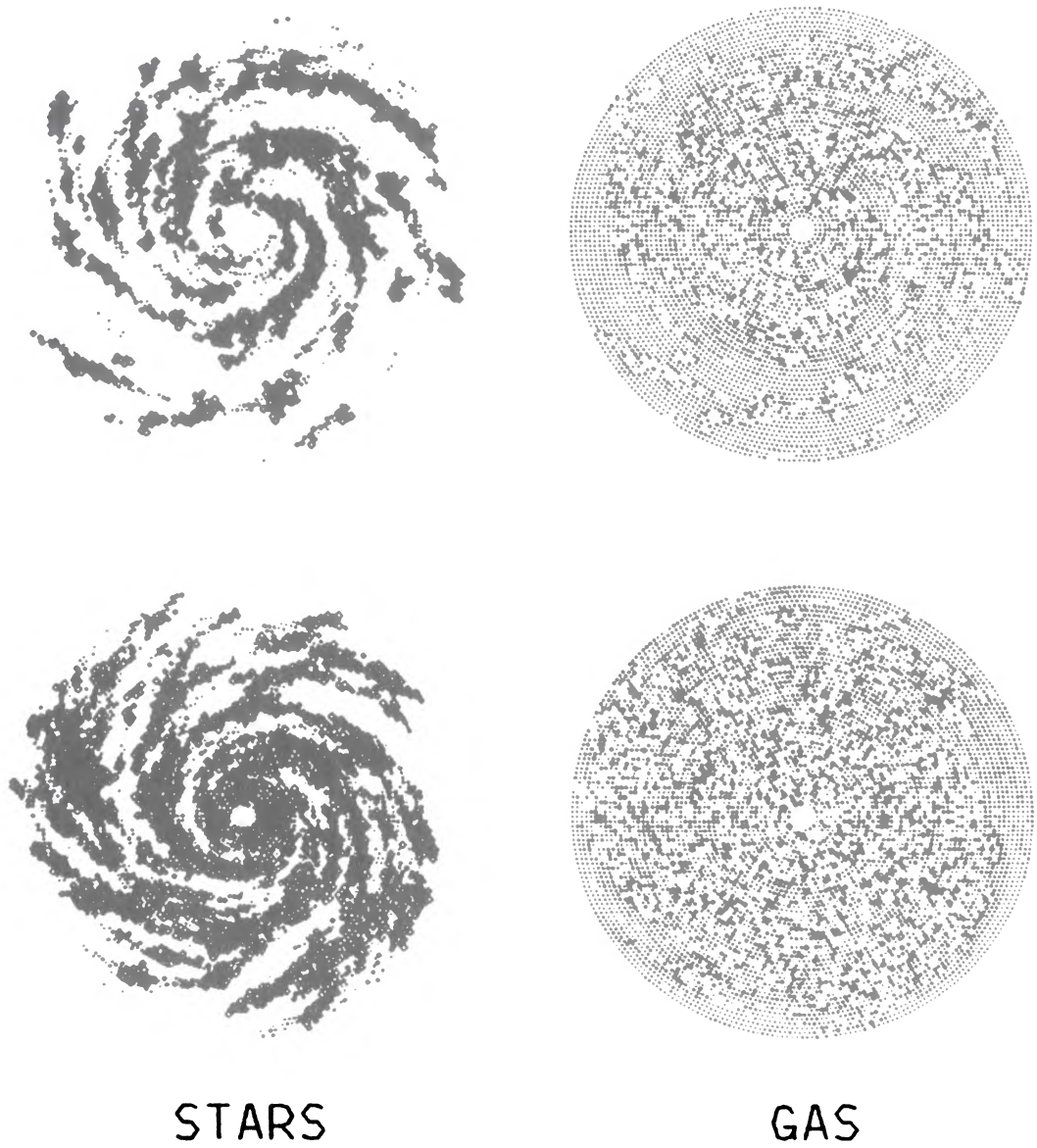

FIG. 9.—Distribution of stars and gas for a stochastic, self-propagating, star-formation model incorporating the interaction between gas and the star-formation process.

arms is not necessarily evidence for the existence of a spiral density wave.

VI. CONCLUSIONS

It was shown in Paper I that the SSPSF model can generate realistic looking galaxies; however, it remained to be demonstrated that the model can give a complete description of the many observed properties of galaxies. In this paper we have begun to consider some of these observations. First, we have shown that the model is capable of directly producing the observed correlation of morphological type with rotational velocity. Second, we find that the appearance of our model galaxies in the various photometric bands agrees quite well with observations. Third, although we have not been able to evaluate quantitatively the integrated colors and fractional gas-mass of galaxies, we have shown that the SSPSF model does provide the proper functional dependence of relative star-formation rate necessary to qualitatively account for the observed correlation of color and gas fraction with morphological type. Last, we have extended the model to take into account the distribution of gas and have shown that it is also possible to obtain spiral arms in the gas.

As mentioned in the introduction, we take these results to imply that many of the properties of spiral

galaxies depend on the nature of the major mode of star formation, which we identify with the SSPSF model, and not on the details of the physics of star formation. In closing, we want to note that this same point can be argued from a purely observational point of view. The observed correlations between morphological type and the different integral properties discussed above appear to be valid for objects with presumably very different dynamics. For example, de Vaucouleurs (1976) pointed out that the color-type relation does not differentiate between normal and barred spirals. Furthermore, Peterson and Shostak (1974) have shown that the fractional gas content, and mass-to-luminosity ratio, of a sample of Arp's "peculiar" spiral galaxies obey quantitatively the same relation to type as "normal" isolated galaxies. It appears then that the rate of the star formation rides on top of the dynamic detailed structure of the spiral galaxies but does not depend strongly on it. We may tentatively conclude on the basis of the results of this paper that the SSPSF mechanism plays a major role in star formation in spiral galaxies.

We are very grateful to Dr. G. de Vaucouleurs for extensive discussions of the correlation of morphological type with various observed properties of galaxies. We also want to thank Drs. F. N. Bash, J. S. Buff, J. M. Huntley, G. L. Lasher, K. H. Prendergast, E. E. Salpeter, C. Struck-Marcel, B. M. Tinsley, and C. Yuan for many important discussions and comments.

REFERENCES

Audouze, J., and Tinsley, B. M. 1976, *Ann. Rev. Astr. Ap.*, **14**, 43.
Brosche, P. 1971, *Astr. Ap.*, **13**, 293.
Burton, W. B. 1976, *Ann. Rev. Astr. Ap.*, **14**, 275.
de Vaucouleurs, G. 1976, *Le Monde des Galaxies* (Besançon: Observatoire de Besançon).
———. 1977, in *The Evolution of Galaxies and Stellar Populations*, ed. B. M. Tinsley and R. B. Larson (New Haven: Yale University Observatory), p. 43.
Dzigvashvili, R. M., and Borchkhadze, T. M. 1970, in *The Spiral Structure of Our Galaxy*, ed. W. Becker and G. Contopoulos (Dordrecht: Reidel), p. 41.
Frogel, J. A., Persson, S. E., and Aaronson, M. 1977, *Ap. J.*, **213**, 723.
Gerola, H., and Seiden, P. E. 1978, *Ap. J.*, **223**, 129 (Paper I).
Hodge, P. 1974, *Pub. A.S.P.*, **86**, 845.
Knapp, G. R., Tremaine, S. D., and Gunn, J. E. 1978, *A.J.*, **83**, 1585.
Kormendy, J., and Norman, C. A. 1979, *Ap. J.*, in press.
Larson, R. B., and Tinsley, B. M. 1978, *Ap. J.*, **219**, 46.
Peterson, S. D., and Shostak, G. S. 1974, *A.J.*, **79**, 767.
Roberts, M. 1975, in *Galaxies and the Universe*, ed. A. Sandage, M. Sandage, and J. Kristian (Chicago: University of Chicago Press), p. 309.
Rubin, V. C., Ford, W. K., Jr., and Thonnard, N. 1978, *Ap. J. (Letters)*, **225**, L107.
Schulman, L. S., and Seiden, P. E. 1978, *J. Stat. Phys.*, **19**, 293.
Schweizer, F. 1976, *Ap. J. Suppl.*, **31**, 313.
Searle, L., Sargent, W. L., and Bagnuolo, W. G. 1973, *Ap. J.*, **179**, 427.
Seiden, P. E., Schulman, L., and Gerola, H. 1979, *Ap. J.*, in press.
Struck-Marcel, C., and Tinsley, B. M. 1978, *Ap. J.*, **221**, 562.
Talbot, R. J., Jensen, E. B., and Dufour, R. J. 1978, preprint.
Tinsley, B. M., and Gunn, J. E. 1976, *Ap. J.*, **203**, 52.

H. Gerola and P. E. Seiden: IBM Thomas J. Watson Research Center, P.O. Box 218, Yorktown Heights, NY 10598